

EFFECTS OF STRONG MAGNETIC FIELDS IN NEUTRON STAR AND GRAVITATIONAL WAVE EMISSION

G. F. MARRANGHELLO

*Physics Institute, Universidade Federal do Rio Grande do Sul, Porto Alegre, Brazil
gfm@if.ufrgs.br*

I review in this work the properties of nuclear and quark matter equation of state under the influence of a strong magnetic field. We analyse the results when they are applied to compact stars description. Finally, we describe the emission of gravitational wave from a compact star that goes over a phase transition.

1 Introduction

The determination of the nuclear matter equation of state and the appearance of new phases at high densities is one of the main goals in present nuclear physics. Nowadays, huge recently planned experiments have brought excellent expectations on these determinations. RHIC and LHC are the most promising tools for direct observations of the high density matter behaviour, from heavy ion collisions. Another important experiments are linked to the observation of neutron star properties, once they are believed to behave like giant hypernucleus and/or giant quark bags. In this direction, Chandra X-Ray Observatory and BeppoSax have done an excellent job analysing the data originated by X-Ray or thermal emission from pulsars. We emphasize the data that indicates important results about more massive neutron stars ($M \sim 2.0-2.2M_{\odot}$) and others about smaller stars with radius $\sim 30\%$ smaller than ordinary neutron star radius. New astrophysical tools are related to the emission of gravitational waves from these extremely dense objects and shall be observed by the american LIGO or by the french-italian collaboration VIRGO.

Such a variety of experiments being located for the seek of nuclear matter equation of state and the quark-gluon plasma phase transition implies in a large amount of theoretical works which are capable to improve the experiments capabilities, direct them to better targets and have their payback with results that may prove theories. Nowadays one can find different works described in many papers, not only because of theoretical physicist's creativity but also because of the many different approaches high energy physics support. One can go from the complex analytical quantum chromodynamics (QCD), step on the lattice simulations, drive through feynman diagrams, and get wherever he wants. They all are valid and the scope of this work do not

include a discussion of the best way of doing nuclear physics or the best model to fit the bulk properties of matter. We intend to use a quantum hydrodynamics (QHD)¹ based model and the MIT² bag model to describe compact stars main properties and trace a consistent path from bulk nuclear matter description to neutron star properties and the gravitational wave emission.

2 Nuclear Matter Equation of State

One consistent, well based and effective model to describe nuclear matter is based on the pioneered work by Walecka which consists one of the basis of nuclear matter effective field theory. Further developments were done by many authors from whose we extract the works by Boguta and Bodmer³, Zimanyi and Moszkowski⁴ and Taurines et. al.⁵, developed in the following years.

We have used the model as described by the lagrangian density below

$$\begin{aligned}
\mathcal{L} = & \sum_B \bar{\psi}_B [i\gamma_\mu (\partial^\mu - g_\omega B \omega^\mu) - (M_B - g_\sigma B \sigma)] \psi_B \\
& - \sum_B \bar{\psi}_B \left[\frac{1}{2} g_\rho B \boldsymbol{\tau} \cdot \boldsymbol{\rho}^\mu \right] \psi_B + \frac{bM}{3} \sigma^3 + \frac{c}{4} \sigma^4 \\
& + \frac{1}{2} (\partial_\mu \sigma \partial^\mu \sigma - m_\sigma^2 \sigma^2) - \frac{1}{4} \omega_{\mu\nu} \omega^{\mu\nu} + \frac{1}{2} m_\omega^2 \omega_\mu \omega^\mu \\
& - \frac{1}{4} \boldsymbol{\rho}_{\mu\nu} \cdot \boldsymbol{\rho}^{\mu\nu} + \frac{1}{2} m_\rho^2 \boldsymbol{\rho}_\mu \cdot \boldsymbol{\rho}^\mu \\
& + \sum_l \bar{\psi}_l [i\gamma_\mu \partial^\mu - M_l] \psi_l .
\end{aligned} \tag{1}$$

which includes the baryonic octet (p, n, $\Lambda, \Sigma^+, \Sigma^0, \Sigma^-, \Xi^-, \Xi^0$) coupled to mesons (σ, ω, ρ), and free leptons (e, μ). The scalar and vector coupling constants, g_σ, g_ω and the coefficients b, c are determined through the nuclear matter bulk properties fitting, i. e., binding energy E_b (= -16.3 MeV), compression modulus K (= 240 MeV) and effective nucleon mass $M^* = M - g_\sigma \bar{\sigma}$ (= 732 MeV) at saturation density ρ_0 (= 0.153 fm⁻³). The g_ρ coupling constant is determined through the nuclear matter asymmetry coefficient, a_4 (= 32.5 MeV). All the coefficient values are described in ref.^{6,7}.

Applying standard technics of field theory and solving the equations at a mean-field level one can extract expressions for the thermodynamical quantities of pressure, p , energy density, ϵ etc. and verify the suitability of this model results to the experimental values of compression modulus, K and effective nucleon mass, M^* , resulting in excellent results for neutron star masses and

radii, which can be compared to previous works^{8,6}. In figure 1 we describe the behaviour of the density of each different particle described by the model as a function of the total baryon density.

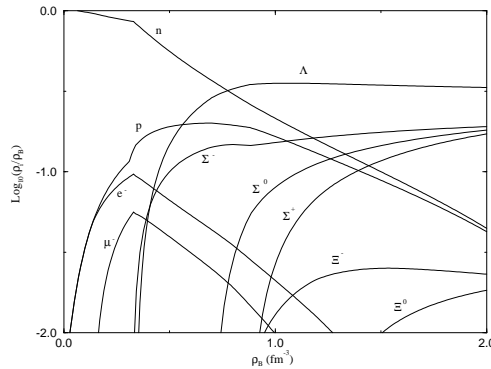


Figure 1. Particle distribution as function of baryon density.

3 Phase Transition to Quark Matter

The nuclear to quark matter phase transition is expected to occur at high densities and/or high temperatures, restoring the chiral symmetry. We follow in this section the work by Heiselberg and Hjorth-Jensen⁹ who perfectly described the conditions for the occurrence, or not, of a mixed phase composed by hadrons and deconfined quarks simultaneously. First claimed by Glendenning¹⁰, the occurrence of a mixed phase where quark structures are immersed into a hadron matter (or vice-versa at higher densities), is now uncertain. This work will not clarify this topic, once it is model-dependent, however, as an application of this study we intend to propose the possible difference on the detection of such phases inside hybrid stars.

Generally, the properties of the transitions with one or more than one conserved charges are quite different. The most important feature is that pressure may be constant or vary continuously with the proportion of phases in equilibrium. Reviewing Heiselberg's work, one can search the answer of which kind of transition is more energetically favored through an analysis of the bulk energy gained in such a transition and the Coulomb and the surface energy relation, as we stress below.

Assuming the model described in the previous section and the MIT bag model for the quark matter,

$$\begin{aligned}
\Omega = & \sum_{q=u,d,s} \frac{-1}{4\pi^2} \left[\mu_q k_{Fq} (\mu_q^2 - \frac{5}{2} m_q^2) + \frac{3}{2} m_q^4 \ln \left(\frac{\mu_q + k_{Fq}}{m_q} \right) \right] \\
& + \frac{2\alpha_c}{4\pi^3} \left[3 \left[\mu_q k_{Fq} - m_q^2 - m_q^2 \ln \left(\frac{\mu_q + k_{Fq}}{m_q} \right) \right]^2 - 2k_{Fq}^4 - 3m_q^4 \ln^2 \left(\frac{m_q}{\mu_q} \right) \right] \\
& \times \left[6 \ln \left(\frac{\rho_r}{\mu_q} \right) \left(\mu_q k_{Fq} m_q^2 - m_q^4 \ln \left(\frac{\mu_q + k_{Fq}}{m_q} \right) \right) \right] + B, \tag{2}
\end{aligned}$$

where Ω is the thermodynamical potential for the MIT bag model, we relate the energy densities in order to calculate the bulk energy. Giving the large uncertainties in the estimates of bulk and surface properties, one cannot claim that droplet phase is favored or not, once it depends crucially on nuclear and quark matter properties.

If droplet sizes and separations are small compared with Debye screening lengths, the electron density will be uniform to good approximation, and the Debye screening length λ_D is defined by

$$\frac{1}{\lambda_D^2} = 4\pi \sum_i Q_i^2 \left(\frac{\partial n_i}{\partial \mu_i} \right)_{n_j, j \neq i} \tag{3}$$

where n_i , μ_i and Q_i are the number density, chemical potential and charge of particle species i .

In the system we consider, screening effects can be estimated and, if the characteristic spatial scales of structures are less than about 10 fm for the nuclear phase, and less than about 5 fm for the quark phase, screening effects will be unimportant, and the electron density will be essentially uniform. In the opposite, the total charge densities in bulk nuclear and quark matter will both vanish.

When quark matter occupies only a small fraction, $f = \frac{V_{QM}}{V_{QM} + V_{NM}}$, of the total volume, quarks will form spherical droplets. The surface energy per droplet is given by $\epsilon_S = \sigma 4\pi R^2$, where σ is the surface tension, and the Coulomb energy is

$$\epsilon_C = \frac{16\pi^2}{15} (\rho_{QM} - \rho_{NM})^2 R^5. \tag{4}$$

Minimizing the energy density with respect to R one obtain the usual result $\epsilon_s = 2\epsilon_C$ and find a droplet radius

$$R = \left(\frac{15}{8\pi} \frac{\sigma}{(\rho_{QM} - \rho_{NM})^2} \right)^2. \quad (5)$$

Our results, considering the models described before, cannot be definitive before a high precise determination of the surface tension, σ . However, for $\sigma \sim 70-100 \text{ MeV}$, a mixed phase is unfavored and the star will have a density discontinuity. The result is a larger radius to support the mixed phase and the equation of state for the constant pressure phase transition is presented below.

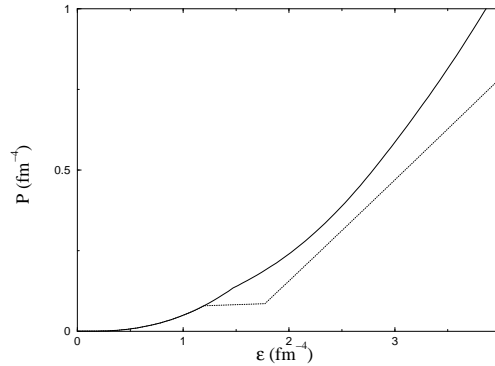


Figure 2. Equation of state for pure neutron star matter (solid line) and for the transition to quark matter (dotted line).

4 Magnetic Field Effects

Several independent arguments link the class of *Soft γ -Ray Repeaters* (SGRs) and perhaps anomalous X-ray pulsars with neutron stars having ultra strong magnetic fields. In addition, two of four known SGRs directly imply, from their periods and spin-down rates, surface fields in the range $2 - 8 \times 10^{14} G$. The magnitude of the magnetic field strength needed to dramatically affect neutron star structure and an estimate done by Lai and Shapiro¹¹ yields $B \sim 2 \times 10^{18} \frac{M/1.4M_{\odot}}{(R/10km)^2}$ in the interior of neutron stars.

In this section we investigate the effects of very strong magnetic fields upon the equation of state of dense matter in which hyperons and quarks are present. In the presence of a magnetic field, the equation of state above nuclear

saturation density is significantly affected both by Landau quantization and magnetic moment interactions, but only for fields strengths $B > 10^{18}G$.

The previously presented lagrangian density in section 2 can be re-written in order to include the magnetic field as

$$\begin{aligned}
\mathcal{L} = & \sum_B \bar{\psi}_B [i\gamma_\mu \partial^\mu - (M_B - g_{\sigma B}^* \sigma) - g_{\omega B}^* \gamma_\mu \omega^\mu + q_b \gamma_\mu A^\mu \\
& - \kappa_b \sigma_{\mu\nu} F^{\mu\nu}] \psi_B - \sum_B \psi_B [\frac{1}{2} g_{\rho B}^* \gamma_\mu \boldsymbol{\tau} \cdot \boldsymbol{\rho}^\mu] \psi_B \\
& + \sum_\lambda \bar{\psi}_\lambda [i\gamma_\mu \partial^\mu - m_\lambda + q_l \gamma_\mu A^\mu] \psi_\lambda \\
& + \frac{1}{2} (\partial_\mu \sigma \partial^\mu \sigma - m_\sigma^2 \sigma^2) - \frac{1}{4} \Omega_{\mu\nu} \Omega^{\mu\nu} - \frac{1}{4} F_{\mu\nu} F^{\mu\nu} \\
& + \frac{1}{2} m_\omega^2 \omega_\mu \omega^\mu - \frac{1}{4} \boldsymbol{\rho}_{\mu\nu} \cdot \boldsymbol{\rho}^{\mu\nu} + \frac{1}{2} m_\rho^2 \boldsymbol{\rho}_\mu \cdot \boldsymbol{\rho}^\mu.
\end{aligned}$$

For detailed and well founded texts on magnetic field effects the authors recommend ref.^{12,13}, from where one can find the energy spectrum for the protons given by

$$\begin{aligned}
E_p = & \sqrt{k_z^2 + \left(\sqrt{M_p^{*2} + 2 * (n + \frac{1}{2} + \frac{s}{2}) q_p B + s \kappa_p B} \right)^2} \\
& + g_\omega \omega_0 - \frac{1}{2} g_\rho \rho_0.
\end{aligned} \tag{6}$$

In a strong magnetic field, particles motion is perpendicular to the field lines and are quantized to give discrete *Landau orbitals*, and the particles behave like a one-dimensional gas rather than a three-dimensional gas and, the higher is the field, the lower is the number of occupied *Landau levels*. The energy of a charged particle changes significantly in the quantum limit if the magnetic field $H \geq H_c$. For electrons, $H_c \sim 4 \times 10^{13}G$, u and d (massless quarks), $H_c \sim 4 \times 10^{15}G$, s -quark, $H_c \sim 10^{18}G$ and protons, $10^{20}G$.

Considering the phase transition aspects, a strong magnetic field unfavors the mixed hadron-quark phase once it increases the electron number in the nuclear phase leaving the quark phase practically unchanged. This increases the droplet size as it was discussed in the previous session and in ref.¹⁴.

5 Compact Stars

The first step through an analysis of compact stars recall the simpler solution to the general relativistic Einsteins equations which represents the static and spherical symmetric stars, the Schwarzschild solution, written as the Tolman-Oppenheimer-Volkoff equations^{15,16}. The TOV equations describe the structure of a static, spherical and isotropic star wit the pressure $p(r)$ and the energy density $\epsilon(r)$ reflecting the underlying nuclear model. The TOV equations involve various constraints and boundary conditions: they must be evaluated for the initial condition $\epsilon(0) = \epsilon_c$ (with ϵ_c denoting the central density) and $M(0) = 0$ at $r = 0$; the radius R of the star is determined under the condition that on its surface the pressure vanishes, $p(r)|_{r=R} = 0$.

The condition for chemical equilibrium for neutron stars are:

$$\mu_i = b_i \mu_n - q_i(\mu_\ell) \quad (7)$$

where μ_i and μ_ℓ stand for the baryon and lepton chemical potentials, respectively; b_i is the baryon number and the baryon and lepton electrical charges are represented by q_i .

The corresponding equations for baryon number and electric charge conservation are:

$$\rho_{baryonic} = \sum_B \frac{k_{F,B}^3}{3\pi^2}, \quad (8)$$

and

$$\sum_B q_{e,B} \frac{k_{F,B}^3}{3\pi^2} - \sum_\ell \frac{k_{F,\ell}^3}{3\pi^2} = 0. \quad (9)$$

Here one can visualize the importance and the effects of quark and nuclear matter parameters determination, once they will have reflects on the properties of compact stars. First, quark stars maximum mass and radius are directly governed by the value of the bag constant as:

$$M = \frac{1.964M_\odot}{\sqrt{B_{60}}} \quad R = \frac{10.71km}{\sqrt{B_{60}}}, \quad (10)$$

where $B_{60} = B/(60MeV/fm^3)$ in the massless quarks case. In the same sense, the strong coupling constant α_c is related to the quark star properties. Both B and α_c will determine whether or not the hadron-quark phase transition will take place. The sequence of neutron stars (mass-energy density relation) and the energy density in the interior of a neutron star is presented in the figures below.

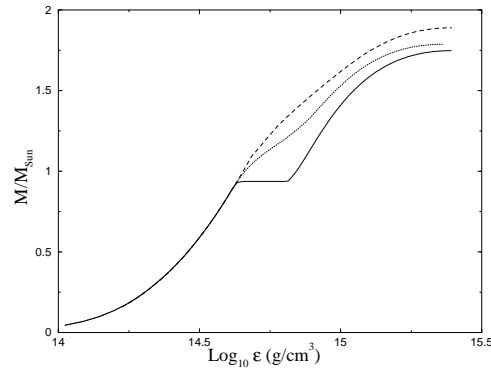


Figure 3. Masses of neutron star as a function of central energy density. The hybrid star without mixed phase (solid line), with mixed phase (dotted line) and the pure neutron star (dashed line) are presented.

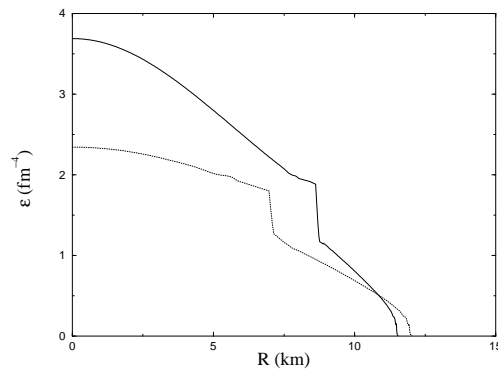


Figure 4. Energy density distribution inside the neutron star for two different central energies.

The nuclear matter coupling constants $g_{B\sigma}$, $g_{B\omega}$ and $g_{B\rho}$ present the same sensibility and uncertainties. Nuclear matter results for effective mass compression modulus and particle distribution play also an important role on the phase transition and star properties and, consequently, on the emission of gravitational wave as we will discuss in the following sections.

The magnetic field effects are presented in the following figures of equation of state, neutron star masses and particle distribution.

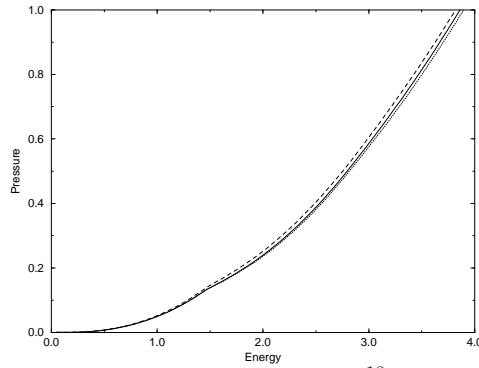


Figure 5. Equation of state at $B=0$ (solid line) and $B=10^{18}$ G with (dotted line) and without (dashed line) the effects of anomalous magnetic moment.

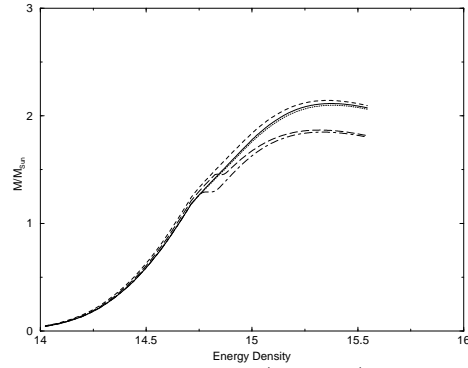


Figure 6. Masses of pure neutron star at $B=0$ (solid line) and $B=10^{18}$ G with (dotted line) and without (dashed line) the effects of anomalous magnetic moment and the masses of hybrid stars at $B=10^{18}$ G (long dashed line) and $B=5 \times 10^{18}$ G (dot-dashed line) as functions of central energy density.

6 The Conversion of Neutron Stars to Hybrid Stars

The transition from configuration H to HQ may occur through the formation of a metastable core, built up by an increasing central density. The increase in the central density may be a consequence of a continuous spin-down or other different mechanisms the star could suffer. This transition releases energy, exciting mainly the radial modes of the star. These modes do not emit GWs,

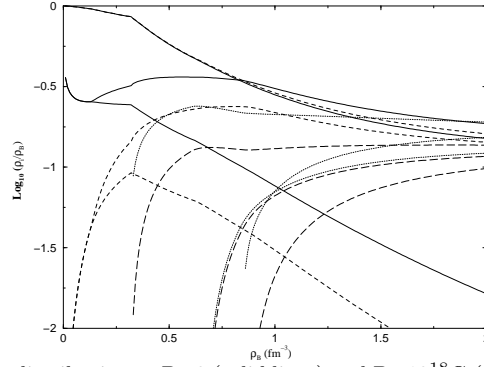


Figure 7. Particles distribution at $B=0$ (solid lines) and $B=10^{18}\text{G}$ (dotted line) as functions of the baryonic density.

unless when coupled with rotation, a situation which will be assumed here.

Strange matter is assumed to be absolutely stable and a seed of strange matter in a neutron star would convert the star into a hybrid or strange star. The speed at which this conversion occurs was calculated by Olinto¹⁷, taking into account the rate at which the down- and strange-quark Fermi seas equilibrate via weak interactions and the diffusion of strange-quarks towards the conversion front.

Accordingly to¹⁷, cold neutron stars can convert to strange star matter with speeds ranging from 5km/s to $2 \times 10^4\text{km/s}$. The outcome of such an event would emit an incredible amount of energy in 0.5ms to 2s . We apply this discussion to the partial conversion of a neutron star to strange matter, forming a hybrid star.

However, the emission of a gravitational wave, which will be discussed in the next section, can only *recognize* the phase transition after a structural rearrangement of the star, which shall reduce its radius and gravitational mass, conserving its total baryon number. Such mechanism has already been studied by Bombaci¹⁸ for the emission of γ -ray bursts.

7 Gravitational Wave Emission

In order to simplify our analysis, we will consider that most of the mechanical energy is in the fundamental model. In this case, the gravitational strain amplitude can be written as

$$h(t) = h_0 e^{-(t/\tau_{gw} - i\omega_0 t)} \quad (11)$$

where h_0 is the initial amplitude, ω_0 is the angular frequency of the mode and τ_{gw} is the corresponding damping timescale. The initial amplitude is related to the total energy E_g dissipated under the form of GWs by the relation¹⁹

$$h_0 = \frac{4}{\omega_0 r} \left[\frac{GE_g}{\tau_{gw} c^3} \right]^{1/2} \quad (12)$$

where G is the gravitational constant, c is the velocity of light and r is the distance to the source.

Relativistic calculations of radial oscillations of neutron star with a quark core were recently performed by Sahu et al.²⁰. However, the relativistic models computed by those authors do not have a surface of discontinuity where an energy jump occurs. Instead a mixing region was considered, where the charges (electric and baryonic) are conserved globally but not locally¹⁰. Oscillations of star models including an abrupt transition between the mantle and the core were considered by Haensel²¹, Miniutti²² and Marranghello⁷. However a Newtonian treatment was adopted and the equation of state used in the calculations does not correspond to any specific nuclear interaction model. In spite of these simplifications, these hybrid models suggest that *rapid* phase transitions, as that resulting from the formation of a pion condensate, proceed at the rate of strong interactions and affect substantially the mode frequencies. However, the situation is quite different for *slow* phase transitions (the present case), where the mode frequencies are quite similar to those of a *one-phase* star²¹. In this case, scaling the results of ²¹, the frequency of the fundamental mode (uncorrected for gravitational redshift) is given approximately by

$$\nu_0 \approx 63.8 \left[\frac{(M/M_\odot)}{R^3} \right]^{1/2} \text{ kHz} \quad (13)$$

where the mass is given in solar units and the radius in km.

Once the transition to quark-gluon matter occurs, the weak interaction processes for the quarks u , d and s

$$u + s \rightarrow d + u \quad \text{and} \quad d + u \rightarrow u + s \quad (14)$$

will take place. Since these reactions are relatively slow, they are not balanced while the oscillations last and thus, they dissipate mechanical energy into heat²³. According to calculations of reference [21], the dissipation timescale can be estimated by the relation

$$\tau_d \approx 0.01 \left(\frac{150 \text{ MeV}}{m_s} \right)^4 \left(\frac{M_\odot}{M_c} \right) \text{ s} \quad (15)$$

where m_s is the mass of the s-quark in MeV and M_c is the mass of the deconfined core in solar masses. This equation is valid for temperatures in the range $10^8 - 10^9 K$. On the other hand, the damping timescale by GW emission is

$$\tau_{gw} = 1.8 \left(\frac{M_\odot}{M} \right) \left(\frac{P_{m.s}^4}{R^2} \right) s \quad (16)$$

where again the stellar mass is in solar units, the radius is in km and the rotation period P is in milliseconds.

In a first approximation, the fraction of the mechanical energy which will be dissipated under the form of GWs is $f_g = \frac{1}{(1+\tau_{gw}/\tau_d)}$. Notice that the damping timescale by GW emission depends strongly on the rotation period. Therefore one should expect that slow rotators will dissipate mostly of the mechanical energy into heat. In table 4 is given for each star model the expected frequency of the fundamental mode (corrected for the gravitational redshift), the critical rotation period (in ms) for having $f_g = 0.50$, the GW damping for this critical period and the quality factor of the oscillation, $Q = \pi\nu_0\tau_{gw}$.

Considering now a strongly magnetized neutron star whose $B \sim 10^{18} G$, we detect an increasing in the gravitational mass of a star composed by pure hadronic matter. However, the gravitational mass of hybrid stars decrease for the case of increasing magnetic field and the explanation is quite simple: once the hybrid star has lower gravitational mass than the pure hadronic one, due to the presence of a softer quark matter in its inner shells and, the phase transition from hadron to quark matter occurs at lower densities with higher magnetic fields, the highly magnetized hybrid star will have a more important quark-gluon plasma core and a lower mass. This fact will represent a larger energy released during the phase transition and gravitational wave emission which could be detected from larger distances.

After filtering the signal, the expected signal-to-noise ratio is

$$(S/N)^2 = 4 \int_0^\infty \frac{|\tilde{h}(\nu)|}{S_n(\nu)} d\nu \quad (17)$$

where $\tilde{h}(\nu)$ is the Fourier transform of the signal and $S_n(\nu)$ is the noise power spectrum of the detector. Performing the required calculations, the S/N ratio can be written as

$$(S/N)^2 = \frac{4}{5} h_0^2 \left(\frac{\tau_{gw}}{S_n(\nu_{gw})} \right) \frac{Q^2}{1+4Q^2} \quad (18)$$

Table 1. Oscillation parameters for $B=0$: the damping timescale τ_{gw} is given for the critical period; maximum distances for VIRGO (V) and LIGO II (L) are in Mpc, and the LIGO II result for $B=10^{18}G$.

ν_0 (kHz)	P_{crit} (ms)	τ_{gw} (ms)	Q -	D_{max} (VIRGO)	D_{max} (LIGO II)	D_{max} $B = 10^{18}G$
1.62	1.64	87.0	442	4.9	10.2	11.5
1.83	1.25	27.0	155	6.4	13.5	15.28
2.06	1.13	17.0	110	6.0	12.8	14.48
2.32	1.06	11.5	84	5.1	11.1	12.56
2.72	1.00	8.4	72	3.6	5.7	6.45

In the equation above, the angle average on the beam factors of the detector were already performed.

From eqs.(4) and (11), once the energy and the S/N ratio are fixed, one can estimate the maximum distance D_{max} to the source probed by the detector. In the last two columns of table 4 are given distances D_{max} derived for a signal-to-noise ratio $S/N = 2.0$ and the sensitivity curve of the laser beam interferometers VIRGO and LIGO II. In both cases, it was assumed that neutron stars underwent the transition having a rotation period equal to the critical value.

We emphasize again that our calculations are based on the assumption that the deconfinement transition occurs in a dynamical timescale²⁴. In the scenario developed in ref.¹⁰, a mixed quark-hadron phase appears and the complete deconfinement of the core occurs according to a sequence of quasi-equilibrium states. The star contracts slowly, decreasing its inertia moment and increasing the its angular velocity until the final state be reached in a timescale of the order of 10^5 yr¹⁰. Clearly, in this scenario no gravitational waves will be emitted and this could be a possibility to discriminate both evolutionary paths.

8 Additional Effects

Additional effects and/or scenarios may improve, or not, the detection of gravitational waves from compact stars. An important aspect is related to the colour superconducting phase. As, in principle, this newer phase would turn the equation of state even softer, enlarging the energy release during the astrophysical phase transition, we decide to analyse such a phase.

The superconducting quark phase is described by the thermodynamical potential²⁵

$$\Omega_{CFL} = \Omega_{Free} - \frac{3}{\pi^2} \Delta^2 \mu^2 + B. \quad (19)$$

The resulting equation of state was evaluated in the TOV equations leading to a smaller radius star, as expected, but also to a less massive star, even for the gravitational and for the baryonic mass. This results did not change significantly the properties of gravitational wave emission as we have expected, however, we still expect a better understanding about high-density matter properties to better describe such phase.

The conversion from a neutron star to a strange star, instead of a hybrid star, is a more catastrophic event and may release much more energy, being detectable from longer distances. This kind of transition was studied by Bombaci¹⁸, in order to describe the emission of γ -ray bursts. Applying our results to describe the emission of gravitational waves we got the following results which leads to one of the most promising gravitational wave generators.

Table 2. Properties of a NS \rightarrow SS conversion and the maximum distances for VIRGO (V) and LIGO II (L) are in Mpc

M_{bar}	M_{SS}	R_{SS}	D_{max}^{Virgo}	D_{max}^{Ligo}
1.0749	0.6445	8.40	15.47	34.63
1.3202	0.7804	8.87	20.01	44.79
1.5724	0.9241	9.30	24.27	54.33
1.8342	1.0727	9.68	28.20	63.13
2.1045	1.2210	9.98	32.07	71.79

9 Conclusions

Summarizing, we worked on a nuclear many-body theory with parametrized coupling constants and the MIT bag model. The phase transition from hadron to quark matter was described considering screening effects and the equation of state was determined. We applied the resulting EOS to the TOV equations also considering intense magnetic field effects. These results are according to previous results obtained by many authors. As a tool for gravitational wave

emission, we considered the phase transition occurring inside the compact star obtained from the TOV equations and releasing energy. According to our results, such an event would be detected as far as 13 Mpc without considering magnetic fields and 15 Mpc for compact star with $B=10^{18}$ G. Considering a NS \rightarrow SS transition, we obtained a much larger distance of up to 71 Mpc.

References

1. B.D. Serot, J.D. Walecka, *Adv. Nucl. Phys.* 16:1,327,1986; *Int. J. Mod. Phys.* E6:515-631, 1997.
2. A. Chodos, R. L. Jaffe, K. Johnson, C. B. Thorn and V. F. Weisskopf, *Phys. Rev.* **D9**, 3471 (1974).
3. J. Boguta and A. Bodmer, *Nucl. Phys.* **A292**, 413 (1977).
4. J. Zimanyi and S. A. Moszkowski, *Phys. Rev.* **C42**, 1416 (1990).
5. A.R. Taurines, C.A.Z. Vasconcellos, M. Malheiro, M. Chiapparini, *Phys. Rev.* C63:065801, 2001.
6. G.F. Marranghello, C.A.Z. Vasconcellos, J.A. de Freitas Pacheco, M. Dillig, *Int.J.Mod.Phys.* E11:83-104, 2002.
7. G. F. Marranghello, C. A. Z. Vasconcellos and J. A. de Freitas Pacheco, *Phys. Rev.* **D66**, 064027 (2002).
8. N. K. Glendenning, F. Weber and S. A. Moszkowski, *Phys. Rev.* **C45**, 844 (1992).
9. H. Heiselberg and M. Hjorth-Jensen, nucl-th/9902033.
10. N. K. Glendenning, *Phys. Rev.* **D46**, 1274 (1992).
11. D. Lai and S. Shapiro, *ApJ.* **442**, 259 (1995).
12. A. Broderick, M. Prakash and J. M. Lattimer, astro-ph/0001537.
13. A. Broderick, M. Prakash and J. M. Lattimer, *Phys. Lett.* **B**, 531 (2002) 167..
14. D. Bandyopadhyay, S. Chakrabarty and S. Pal, astro-ph/9703066.
15. R. C. Tolman, *Phys. Rev.* **55**, 364 (1939).
16. J. R. Oppenheimer and G. M. Volkoff, *Phys. Rev.* **55**, 374 (1939).
17. V. Olinto, *Phys. Lett.* **B**, 192 (1987) 71.
18. I. Bombaci, *Lect. Notes in Phys.* **578:Physics of Neutron Star Interiors**, edited by D. Blaschke, N. K. Glendenning, A. Sedrakian (Springer-Verlag, 2001).
19. J. A. de Freitas Pacheco, Proceedings of the VI International Workshop on Relativistic Aspects of Nuclear Physics, ed. T.Kodama et al., World Scientific, 2001, p.158
20. P.K. Sahu and G.F. Burgio and M. Baldo, *ApJ* **566**, L89 (2002).
21. P. Haensel and J.L. Zdunik and R. Schaeffer, *A&A* **217**, 137 (1989).
22. G. Miniutti and J. A. Pons and E. Berti and L. Gualtieri and V.Ferrari, astro-ph/0206142.
23. Qing-de Wang and Tan Lu, *Chin.Astr.Astrophys.* **9**, 159 (1984).
24. P. Haensel and M. Prózyński, *ApJ* **258**, 306 (1982).
25. G. Lugones and J. E. Horvath, *Phys. Rev.* **66**, 074017 (2002).